TECHNIQUES FOR PHYSIOLOGY

A technique for simultaneous measurement of Ca^{2+}, FRET fluorescence and force in intact mouse small arteries

W. Gil Wier, Mark A. Rizzo, Hema Raina and Joseph Zacharia

Department of Physiology, School of Medicine, University of Maryland Baltimore, 655 West Baltimore St, Baltimore, MD 21201, USA

FRET (Forster resonance energy transfer)-based biosensor molecules are powerful tools to reveal specific molecular interactions in cells. Typically however, they are used in cultured cells that (inevitably) express different genes than their counterparts in intact organisms. In such cells it may be impossible to administer physiological stimuli and measure physiological outputs. Here, through the use of transgenic mice that express a FRET-based myosin light chain kinase (MLCK) biosensor molecule, we report a technique for dynamically observing activation and regulation of MLCK within the smooth muscle cells of intact, functioning small arteries, together with measurement of arterial force production and intracellular $[Ca^{2+}]$.

(Received 23 January 2008; accepted after revision 20 March 2008; first published online 27 March 2008)
Corresponding author W. G. Wier: Department of Physiology, School of Medicine, University of Maryland Baltimore, 655 West Baltimore St, Baltimore, MD 21201, USA. Email: gwier001@umaryland.edu

Contraction of smooth muscle is primarily dependent on phosphorylation of myosin regulatory light chains (RLC), as determined by the relative activity of Ca^{2+}–calmodulin (CaM)-dependent myosin light chain kinase (MLCK) and myosin light chain phosphatase (MLCP). In experiments on arteries, it is typical now to measure intracellular $[Ca^{2+}]$ and contraction (force or artery diameter). Yet, as implied above, Ca^{2+} does not uniquely specify force in smooth muscle: several critical processes influence the relationship between Ca^{2+} and force, including: (i) the binding of Ca^{2+} to calmodulin, (ii) activation of MLCK by the binding of Ca^{2+}–CaM, (iii) the actual kinase activity of MLCK, and (iv) the phosphatase activity of MLCP. All of these processes are, of course, themselves subject to regulation.

Study of contractile activation in arterial smooth muscle would be aided greatly by the ability to observe one or more of the processes mentioned above, together with Ca^{2+} and to do so in intact arteries, where physiological stimuli and responses can be obtained. Indeed, a Ca^{2+}–CaM-dependent MLCK 'biosensor' molecule (utilizing FRET) has been constructed recently and expressed specifically in the smooth muscle of (transgenic) mice, permitting for the first time the real-time evaluation of MLCK activation by Ca^{2+}–CaM in response to receptor agonists and depolarization (Isotani *et al.* 2004), and the simultaneous measurement of force (bladder muscle). The FRET signal provides an indication of the conformational change in MLCK that is associated with the binding of Ca^{2+}–CaM, and also of the catalytic (kinase) activity of MLCK (Geguchadze *et al.* 2004). Thus, changes in FRET ratio of the MLCK biosensor might reflect changes in available Ca^{2+}–CaM (which could arise from changes in $[Ca^{2+}]$ or available [CaM]), and/or changes in the affinity of MLCK for Ca^{2+}–CaM, and/or changes in the V_{max} of the reaction. Using these animals, we now report a technique for simultaneous observation of $[Ca^{2+}]$, MLCK activation (FRET), and contraction in intact mesenteric small arteries. To obtain nearly simultaneous observations of $[Ca^{2+}]$ changes and MLCK activation in an artery, we used wide-field imaging of biosensor arteries that had been loaded with fura-2.

Using this technique we obtained evidence that MLCK activity is not the sole determinant of contraction during KCl exposure; a process dependent on *rho*-kinase appears to be activated early during KCL exposure, significantly increasing 'Ca^{2+} sensitivity', probably involving MLCP (Somlyo & Somlyo, 2003). The results also showed that MLCK can be regulated during KCl-induced contraction; presumed elevation of cAMP after activation of adenylate cyclase changed the relationship between intracellular Ca^{2+} and MLCK FRET ratio, consistent with a decreased affinity of MLCK for Ca^{2+}–calmodulin (Nishikawa *et al.* 1984).

Methods

Ethical approval

All experiments were carried out according to the guidelines of the Institutional Animal Care and Use

 DOI: 10.1113/jphysiol.2008.151522

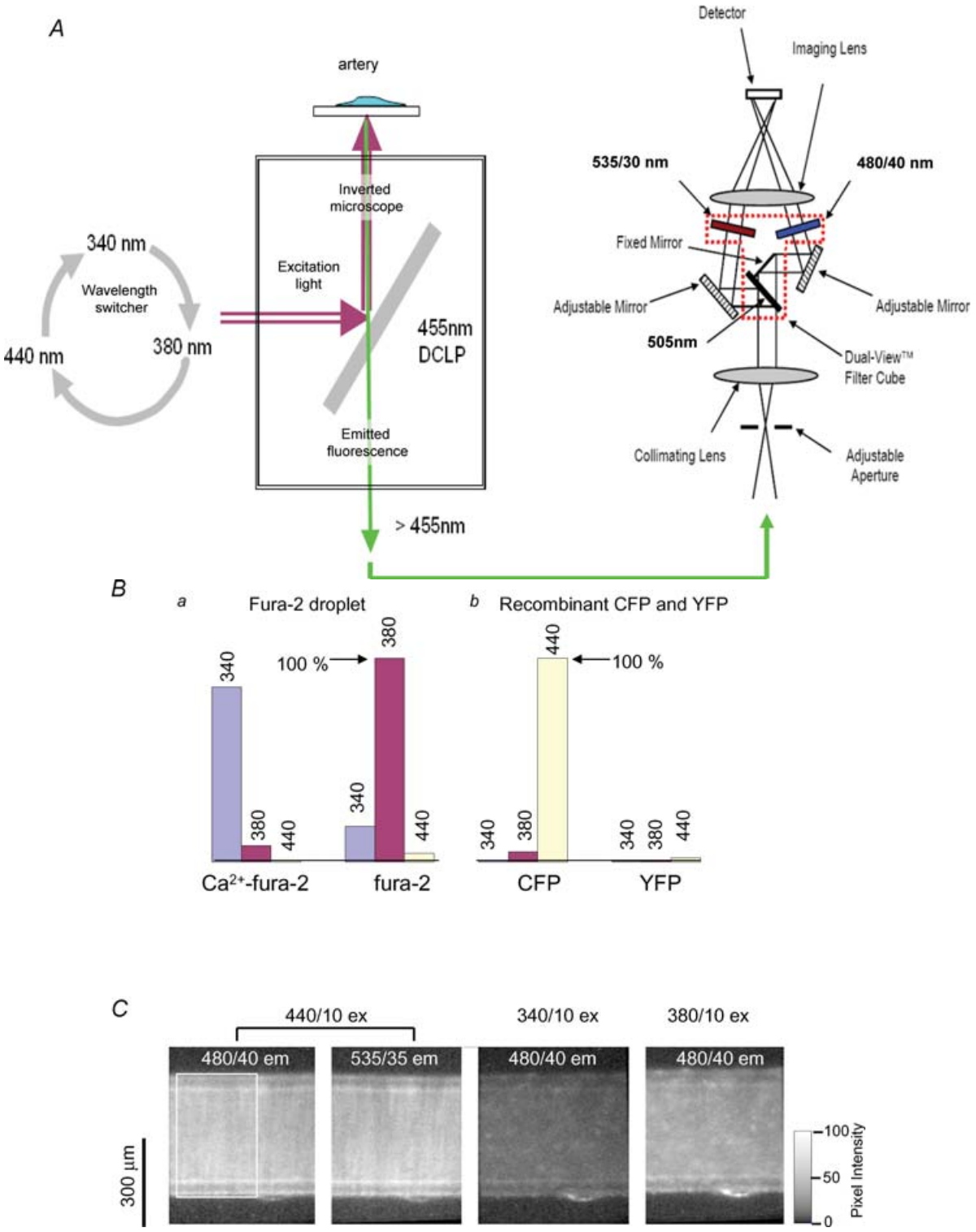

Figure 1. Schematic diagram of fluorescence microscope system for measurement of fura-2 fluorescence and MLCK Biosensor FRET from arteries

A, sequential illumination at the 3 required wavelengths (340 nm, 380 nm, 440 nm) was provided by a high-speed wavelength-switching light source (Lambda DG-4, Sutter Instrument Company, Novato, CA, USA) equipped with a 175 W xenon arc lamp. Light at the selected wavelength was directed to the artery by a Nikon CFI Plan Fluor ELWD 20× C objective lens (n.a.; 0.45). Emitted fluorescence at wavelengths greater than 455 nm was directed into the 'Dual-View' filter cube (Optical Insights LLC, Santa Fe, NM USA). A dichroic mirror (505 nm), fixed mirror and two emission filters (480/40 nm) and (535/35 nm) allowed formation of

Committee of the University of Maryland, School of Medicine. The transgenic mouse line was the same as used previously (Isotani *et al.* 2004), that expresses a MLCK biosensor that monitors the binding of Ca^{2+}–calmodulin through changes in FRET (Forster resonance energy transfer) between cyan fluorescent protein (CFP) and yellow fluorescent protein (YFP). Wild-type and transgenic (TG) mice were maintained on 12 : 12 h light–dark schedule at 22–25°C and 45–65% humidity and fed *ad libitum* on a standard rodent diet and tap water. For these studies, a total of 28 adult mice (28–35 g, 12–18 weeks), were killed by inhalation of CO_2.

Preparation of arteries, solutions and chemicals

The mesenteric arcade was dissected from the abdominal cavity, rinsed free of blood, and placed in a temperature-controlled dissection chamber (5°C) containing a solution of the following composition (mmol l^{-1}): 3.0 Mops, 145.0 NaCl, 5.0 KCl, 2.5 $CaCl_2$, 1.0 $MgSO_4$, 1.0 KH_2PO_4, 0.02 EDTA, 2.0 sodium pyruvate and 5.0 glucose (pH 7.4). Segments of the third order mesenteric arteries 2 mm in length, approximately 250 μm in diameter, were transferred to a recording chamber, where they were mounted on a wire myograph (Danish Myotech Technology, Denmark). If calcium indicators were to be used, the artery was then exposed to dissection solution containing fura-2 AM at 5 μM and loading was allowed to proceed for 1 h at room temperature. After loading was complete or upon beginning the experiment, superfusion was begun with the standard experimental solution containing (mmol l^{-1}): 112.0 NaCl, 25.7 $NaHCO_3$, 4.9 KCl, 2.0 $CaCl_2$, 1.2 $MgSO_4$, 1.2 $KHPO_4$, 11.5 glucose and 10.0 Hepes (pH 7.4, equilibrated with gas of 5% O_2–5% CO_2–90% N_2). Solutions containing elevated KCl were made by replacing the NaCl with KCl on an equimolar basis. The vessels were then normalized at 32°C, that is, the resting tension–internal circumference (IC) relation was determined for each vessel (Mulvany & Halpern, 1977). The IC was set to 90% of that at which the effective resting transmural pressure (ERTP) would be 100 mmHg (13.3 kPa). The inhibitor of *rho*-associated kinase (ROK), Y-27632 [(*R*)-(+)-trans-*N*-(4-pyridyl)-4-(1-aminoethyl)-cyclohexanecarboxanecarboxamide, 2HCl] was obtained from EMD Chemicals (Gibbstown, NJ, USA).

Fluorescence measurements

The methods used to observe [Ca^{2+}] and MLCK FRET were similar to those described recently for the simultaneous measurement of [Ca^{2+}] and cAMP in isolated cells (using a FRET based cAMP sensor similar to the MLCK biosensor used here) (Harbeck *et al.* 2006). Briefly, because of the spectral properties of fura-2 and the MLCK biosensor, it is possible to excite fura-2 and CFP of the MLCK biosensor selectively (at different times, with different excitation filters) and therefore to collect fluorescence emission selectively from each. Since the emission spectrum of fura-2 overlaps entirely that of both CFP and YFP, the emission of fura-2 can be collected with either one (or both together) of the same emission filters that are used for the MLCK biosensor. Thus, there is no need to change or alternate emission filters. In this work, we collected fura-2 fluorescence at 480/40 nm.

For the present experiments, the theory and method of measurement can be summarized as follows: (1) with excitation at 340/10 nm, fura-2 is excited selectively (predominantly the Ca^{2+}-bound form), and fura-2 emission is collected at 480/40 nm; (2) with excitation at 380/10 nm, fura-2 is again excited selectively (predominantly the Ca^{2+}-free form), with fura-2 emission the same; and (3) with excitation at 440/10 nm, CFP of the MLCK biosensor is excited selectively. CFP emission is measured at 480/40 nm, and YFP emission is measured at 535/35 nm. Because of spectral overlap

two separate, spectrally distinct images, one on each side of the detector (XR/Mega-10 intensified CCD camera, Stanford Photonics, Palo Alto, CA, USA). *B*, analysis of efficacy and selectivity of fluorescence excitation of fura-2, CFP and YFP in fluorescence microscope. *Ba*, normalized fluorescence emission (480/40 nm) of droplets of Ca^{2+}–fura-2 and fura-2 (Ca^{2+} free), with excitation at the wavelengths indicated (340/10 nm, 380/10 nm, 440/10 nm). Fluorescence emission of fura-2 (Ca^{2+} free) excited by 440/10 nm is 4.4% of that excited by 380/10 nm; Ca^{2+}–fura-2 is not excited detectably by 440/10 nm. *Bb*, fluorescence excitation of samples of pure enhanced cyan fluorescent protein (CFP, 480/40 nm) and enhanced yellow fluorescent protein (YFP, 535/35 nm). Proteins were bound to agarose beads. Direct emission of YFP is negligible at all excitation wavelengths; fluorescence emission of CFP is excited 5% as effectively by light at 380/10 nm as by light at 440/10 nm. The data show that fura-2 and the MLCK biosensor can each be excited selectively (see text for further analysis). *C*, images of an artery mounted in the fluorescence microscope. The 4 images were derived from 3 successive video frames. The two images labelled '440/10 ex' are from the left and right halves of the first video frame (of a 3 frame sequence), with emission filters of 480/40 nm and 535/35 nm, respectively (see Methods), and are the images of the MLCK biosensor fluorescence in the artery. Image labelled '340/10 ex' is from the left half of the next (2nd of the sequence) video frame (emission filter; 480/40 nm). Image labelled 380/10 ex is from the left half of the next (3rd of the sequence) video frame (emission filter; 480/40 nm). Images are displayed with a non-linear grey scale (at right), in order to facilitate visualization of the fura-2 image with 340 nm excitation, which is relatively dim compared to the others. The white lined box indicates the area of interest (AOI) from which average fluorescence intensity was derived.

of CFP and YFP fluorescence emission, the YFP channel also contains CFP emission amounting to 50% of that measured in the CFP channel, as determined by imaging agarose beads that individually bound either recombinant CFP or YFP (see below), Thus, YFP fluorescence was calculated as YFP = $F_{535} - 0.5$*CFP, where F_{535} symbolizes the total fluorescence in the nominal YFP channel. The emission images were obtained through the use of a 'Dual-View' (Optical Insights, LLC) multicolour imager and an intensified CCD video camera (XR/Mega-10, Stanford Photonics, Inc.). Fluorescence excitation typically followed the sequence 340 nm, 380 nm, 440 nm, with typical exposure times of 0.5 s at each wavelength (Fig. 1*A*).

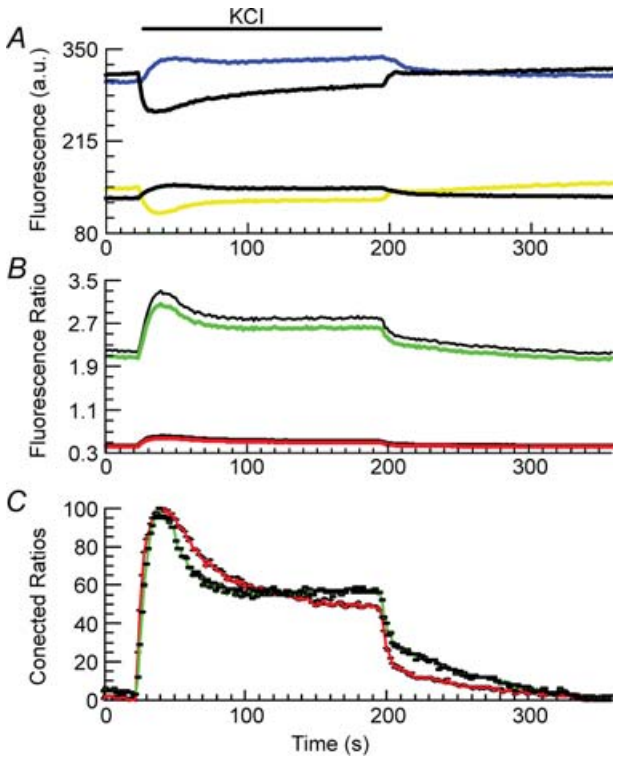

Figure 2. Fluorescence emission of fura-2 and MLCK biosensor from an artery stimulated by KCl (60 mM). MLCK biosensor and fura-2 fluorescence do not interfere with each other
A, blue trace, nominal CFP (440/10 nm excitation, 480/40 nm emission; yellow trace, nominal YFP emission, corrected for CFP component (440/10 nm excitation, 535/35 nm emission); upper black trace, nominal fura-2 emission at 380/10 nm excitation; lower black trace, nominal fura-2 emission with 340/10 nm excitation. *B*, fluorescence ratios; green trace, MLCK FRET ratio, CFP/YFP; black trace, MLCK FRET ratio corrected for fura-2 interference, as described in text; red trace, fura-2 ratio, f2(340)/f2(380), black trace, fura-2 ratio corrected for MLCK interference. *C*, normalized, corrected fluorescence ratios; green trace, corrected MLCK FRET ratio, overplotted black points, uncorrected MLCK FRET ratio; red trace, uncorrected fura-2 ratio, overplotted black points, corrected fura-2 ratio. Although 'correction' for spectral interference shifts the baseline of the fluorescence ratios slightly (*B*), neither the magnitude nor the time course of the changes in MLCK FRET and fura-2 ratios are significantly affected.

Quantitative analysis of fluorescence

Although selective excitation of fura-2 and MLCK biosensor is theoretically possible because their excitation spectra overlap only to a small extent at certain wavelengths, practical evaluation of the efficacy of selective excitation is still required. Even a small overlap of excitation spectra over the particular excitation wavelength band used (10 nm, here) could produce interference, if, for example, one fluorophore was present in much higher concentration than the other, or was much brighter (higher quantum yield), or received much higher excitation intensity. The performance of the system must be evaluated both with fluorescent samples (Fig. 1*B*) and with an artery that contains both fura-2 and MLCK biosensor (Figs 1*C* and 2).

Selective excitation of MLCK biosensor. To evaluate selective excitation of the MLCK biosensor over fura-2, droplets of Ca^{2+}-bound fura-2 and Ca^{2+}-free fura-2 in the specimen plane were illuminated at 340/10 nm, 380/10 nm and 440/10 nm (Fig. 1*Ba*) and emission was collected at 480/40 nm. With 440/10 nm excitation, only Ca^{2+}-free fura-2 is excited to an appreciable extent: 4.4% of that achieved at 380/10 nm. Thus, as an upper limit, when both fura-2 and MLCK biosensor are present, a signal equal to 4.4% of the fura-2 fluorescence (380/10 nm) might be present in the CFP and YFP signals. (The estimate is an upper limit because, in arteries, the fura-2 fluorescence with 380/10 nm illumination is actually only comprised in part by emission from Ca^{2+}-free fura-2; some Ca^{2+}-bound fura-2 is always present, but it is not excited at 440/10 nm.)

Selective excitation of fura-2. To evaluate selective excitation of fura-2 over the MLCK biosensor, we used samples of recombinant CFP and YFP (bound to HiTrap agarose beads, GE Health Care) (Fig. 1*Bb*). In the system used here, CFP is excited only 5.0% as effectively by 380/10 nm as it is by 440/10 nm, and is not excited detectably at 340/10 nm. Thus, only when illuminating at 380/10 nm, is a component of the fluorescence attributed to fura-2 actually due to excitation of the MLCK biosensor (CFP only). This component may be estimated as 5.0% of the measured CFP fluorescence.

Results

Fluorescence emission from an artery containing both fura-2 and MLCK biosensor illuminated at the three wavelengths is shown in Fig. 1*C*. A non-linear grey scale (shown at the right) was used to facilitate visualization of the relatively dim fura-2 image (labelled 340/10 ex) in comparison to the MLCK biosensor fluorescence images. As a wide-field epi-fluorescence microscope was used, spatially resolved images of fluorescence in individual

smooth muscle cells could not be obtained. Accordingly, fluorescence in each image was averaged in a user-selected area of interest (AOI), set to just contain the image of the artery and to exclude any background or other undesired features (Fig. 1*C*). This minimized changes in fluorescence related to contraction and provided an accurate estimate of mean fluorescence within the artery.

Figure 2*A* illustrates the changes in fluorescence within an AOI of a fura-2-loaded, MLCK biosensor artery exposed to elevated KCl (60 mM) during the time indicated. The YFP trace has been corrected for overlapping CFP emission, as described above. Experiments on wild-type arteries not loaded with fura-2 revealed endogenous artery fluorescence which either did not change during exposure to KCl, or which changed in small proportion to recorded force and was cancelled completely in the fluorescence ratios. Thus, the presence of endogenous artery fluorescence affects the absolute values of the fluorescence ratios, but not the changes. We also evaluated the possible effects of the small non-selective excitation of fura-2 and MLCK biosensor that was described above. First, simple fluorescence ratios (F_{340}/F_{380} and CFP/YFP) were calculated as shown in Fig. 2*B* for fura-2 (red) and MLCK biosensor (green). Ratios corrected for non-selective excitation are shown superimposed in black and were calculated as follows, using the parameters determined above:

$$\text{FRET ratio} = (\text{CFP} - 0.044 \times F_{380})/(\text{YFP} - 0.044 \times F_{380})$$

$$\text{Fura-2 ratio} = F_{340}/(F_{380} - 0.050 \times \text{CFP})$$

where F_{340} and F_{380} refer to the fura-2 fluorescence emission at those two excitation wavelengths. Because all the waveforms are similar in shape, the main effect is a small shift in the magnitude of the ratios. There was no detectable effect of correction on the time course of the change in ratios (Fig. 2*C*), where each ratio has been normalized to its maximum change from baseline. The possible significance of the slightly different time

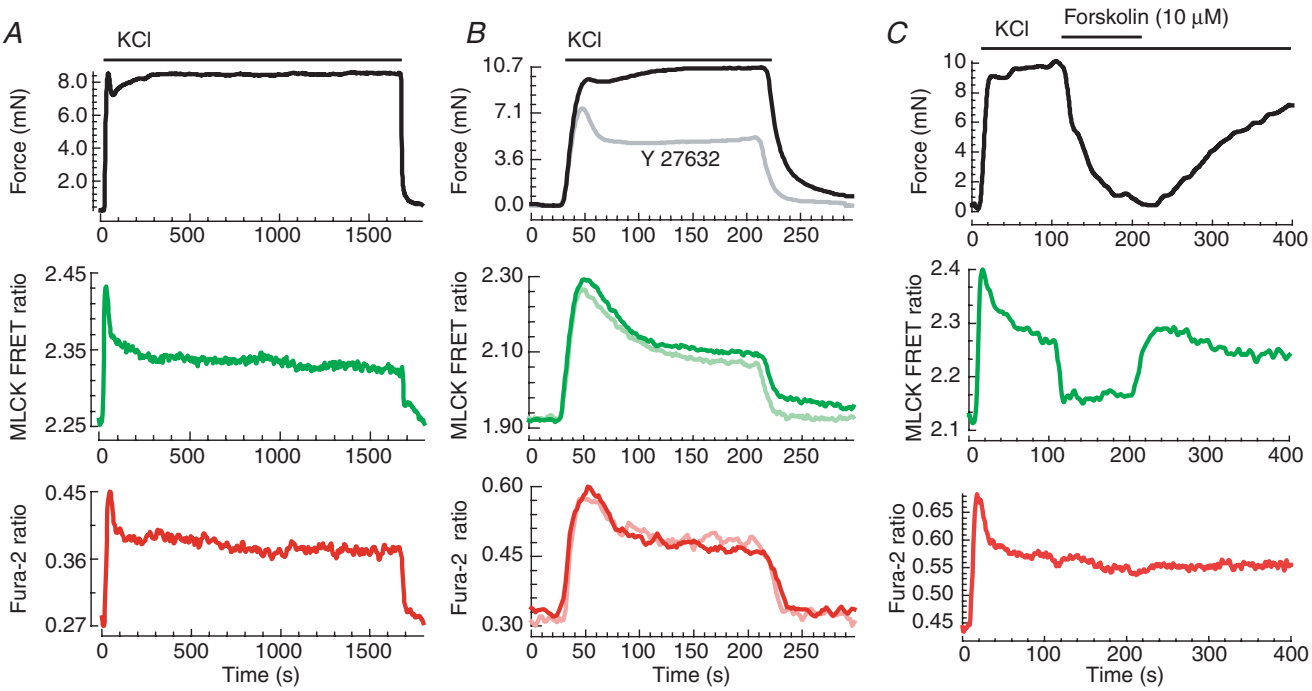

Figure 3. Basic phenomena of changes in [Ca^{2+}], MLCK activation (MLCK FRET ratio) and force in a small artery activated by exposure to elevated [KCl]
A, time course of KCL-induced force (black, upper), MLCK FRET ratio (green, middle) and fura-2 fluorescence (red, lower). After the phasic components, force, MLCK FRET ratio and [Ca^{2+}] are all maintained for the duration of the exposure, nearly 30 min. *B*, Ca^{2+} sensitivity of contraction changes during KCL exposure; *rho*-kinase is activated early during KCl exposure. Pre-incubation with the *rho*-kinase inhibitor Y-27632 (1.0 μM, light coloured lines) strongly reduced maintained force induced by KCl, but had less effect on initial, phasic force, and did not affect MLCK FRET ratio or the Ca^{2+} indicator signal. *C*, forskolin stimulates regulation of MLCK. Forskolin (10.0 μM) was applied during exposure to 60 mM KCl during the time indicated by the black bar. Forskolin caused rapid relaxation of force, and a rapid decrease in MLCK FRET ratio, but no change in the Ca^{2+} indicator signal. The rapid relaxation may be related to the rapid apparent decrease in the affinity of MLCK for Ca^{2+}–calmodulin. The slower, continuing relaxation may be related to other processes, such as regulation of MLCP.

courses of change in MLCK FRET and fura-2 ratios is not known at this time. As will be seen later, the two ratios can diverge to a much larger extent, under other experimental conditions, indicating changes in affinity of MLCK biosensor for Ca^{2+}–CaM. Because the errors in the changes in ratio are essentially undetectable (Fig. 2*C*), ratios were not routinely corrected in this way. Finally, correction for photobleaching of CFP (which bleaches faster than YFP) was not necessary; photobleaching was not significant, as shown by the blue trace in Fig. 2*A*.

MLCK FRET ratio and Ca^{2+} indicator signals during KCL exposure were very similar in time course, both initially and later, reaching steady maintained levels over very long periods of time during KCl exposure (e.g. nearly 30 min, Fig. 3*A*). Although force was similarly maintained, the time course of force initially was quite different from that of MLCK FRET and Ca^{2+} (indicator signal). After the initial, 'phasic' component, force often rose slowly again, during a time when MLCK FRET and Ca^{2+} were declining. This phenomena was typical of all (12) arteries studied with this protocol. Since changes in force were not positively correlated at all times with changes in MLCK activation, one possible mechanism of such a phenomenon would be a decrease in myosin light chain phosphatase activity (i.e. an increase in 'Ca^{2+} sensitivity') as mediated by *rho*-kinase. In three arteries, the *rho*-kinase inhibitor Y-27632 (1.0 μM) reduced the initial transient force to $77.6 \pm 5.4\%$ of control and the steady force to $49.9 \pm 4.8\%$ (Fig. 3*B*), as if a *rho*-kinase-mediated increase in 'Ca^{2+} sensitivity' developed during KCL exposure. The corresponding MLCK FRET ratio and Ca^{2+} indicator signal were not affected significantly. Inhibition of *rho*-kinase thus made the time courses of force, Ca^{2+} and MLCK FRET ratio much more similar to each other, supporting the idea that changes in Ca^{2+} sensitivity mediated by *rho*-kinase are involved even in contraction activated by KCl.

Cyclic AMP (cAMP), produced after β-adrenoceptor (β-AR)-mediated activation of adenylate cyclase (AC), is a particularly important modulator of smooth muscle contractility, acting through cyclic nucleotide-dependent protein kinases (PKA, PKG), and possibly through cyclic nucleotide-activated guanine nucleotide exchange factors (GEFs, such as 'exchange protein directly activated by cAMP' or Epac) (Schmidt *et al.* 2007). When applied during the KCl exposure (Fig. 3*C*), the AC activator forskolin (10.0 μM) caused a rapid relaxation of force, a rapid decrease in MLCK FRET ratio, but no change in Ca^{2+} indicator signal. In six arteries, the MLCK FRET ratio was reduced by forskolin (10.0 μM) to $61.3 \pm 5.6\%$ (mean ± S.E.M.) of the change elicited by KCl. Force, measured at the end of the initial rapid relaxation, was reduced to $73.9 \pm 2.7\%$ of the level prior to forskolin. By the end of the exposure to forskolin, force had fallen to $7.8 \pm 3.4\%$.

Discussion

In this work we have shown that Ca^{2+} indicator signals, force, and FRET signals that reflect conformational changes in genetically encoded exogenous biosensor molecules, can be obtained from intact small arteries of apparently normal, but transgenic, mice. In the case of the MLCK biosensor, this allows a rather direct observation of another link in the chain of events leading from a rise in intracellular [Ca^{2+}] to cross-bridge cycling (force generation). Changes in 'Ca^{2+} sensitivity' are revealed most directly by changes in force without concomitant changes in MLCK activation.

It is known from previous biochemical studies that the affinity of MLCK for Ca^{2+}–calmodulin is regulated by several protein kinases, including protein kinase A (PKA), Ca^{2+}–calmodulin-activated kinase II (CaMK II), protein kinase C (PKC), p21-activated kinase (PAK), and mitogen-activated protein kinase (MAPK) (see Kamm *et al.* 2001 for review). The technique described here should allow determination of the physiological significance of these regulatory pathways, particularly when changes in intracellular [Ca^{2+}] are involved.

In general, we have shown that FRET and other optical signals are readily obtained from arteries of transgenic animals that express these transgenes. Thus, protein activation and regulation may be studied optically, under nearly physiological conditions, provided the appropriate FRET biosensor can be constructed. As currently developed, the technique described here does not provide spatially resolved, calibrated measurements of intracellular [Ca^{2+}] or FRET. There is no reason in principle, however, that the method cannot be extended to confocal microscopy, particularly if the Nipkow spinning disk type is used, in which video cameras are used to capture full-frame images in real-time.

References

Geguchadze R, Zhi G, Lau KS, Isotani E, Persechini A, Kamm KE & Stull JT (2004). Quantitative measurements of Ca^{2+}/calmodulin binding and activation of myosin light chain kinase in cells. *FEBS Lett* **557**, 121–124.

Harbeck MC, Chepurny O, Nikolaev VO, Lohse MJ, Holz GG & Roe MW (2006). Simultaneous optical measurements of cytosolic Ca^{2+} and cAMP in single cells. *Sci STKE* **2006**, l6.

Isotani E, Zhi G, Lau KS, Huang J, Mizuno Y, Persechini A, Geguchadze R, Kamm KE & Stull JT (2004). Real-time evaluation of myosin light chain kinase activation in smooth muscle tissues from a transgenic calmodulin-biosensor mouse. *Proc Natl Acad Sci U S A* **101**, 6279–6284.

Kamm KE & Stull JT (2001). Dedicated myosin light chain kinases with diverse cellular functions. *J Biol Chem* **276**, 4527–4530.

Mulvany MJ & Halpern W (1977). Contractile responses of small arterial resistance vessels in spontaneously hypertensive and normotensive rats. *Circ Res* **41**, 19–26.

Nishikawa M, de Lanerolle P, Lincoln TM & Adelstein RS (1984). Phosphorylation of mammalian myosin light chain kinases by the catalytic subunit of cyclic AMP-dependent protein kinase and by cyclic GMP-dependent protein kinase. *J Biol Chem* **259**, 8429–8436.

Schmidt M, Sand C, Jakobs KH, Michel MC & Weernink PA (2007). Epac and the cardiovascular system. *Curr Opin Pharmacol* **7**, 193–200.

Somlyo AP & Somlyo AV (2003). Ca^{2+} sensitivity of smooth muscle and nonmuscle myosin II: modulated by G proteins, kinases, and myosin phosphatase. *Physiol Rev* **83**, 1325–1358.

Acknowledgements

The MLCK Biosensor mice and constructive comments on the work were generously provided by Professor James T. Stull, The University of Texas Southwestern Medical Center at Dallas, Dallas, TX, USA. Financial support was provided by the National Heart, Lung and Blood Institute (NHLBI) (USA) HL 073094.